lone pairs have much greater s character than N lone pairs and will be more contracted. Second, the P-P distance is about 0.8 Å longer than the N-N distance which keeps the P lone pairs well separated. The HF/6-31G* surface for **23P** does exhibit a *gauche* minimum unlike **23N**. This too is a consequence of diminished lone-pair repulsion in **23P** as compared to **23N**.

The rotational barriers of the unsubstituted phospha-1,3-butadienes examined here are all relatively small (less than 8 kcal mol^{-1}). Stable *gauche* conformers are readily accessible and lie only 1-3 kcal mol^{-1} above the global minimum *trans* conformers. There appears to be no inherent reason the phospha-1,3-butadienes cannot adopt a *gauche* (or even sample the *cis*) conformation that is needed for electrocyclic and cycloaddition reactions to occur. The dearth of reactions of this type for the acyclic phosphabutadienes must therefore arise from another source. One distinct possibility is that the currently produced phosphabutadienes possess large substituents that may sterically prevent the butadiene backbone from attaining the necessary *cis* conformation. Another possibility is that the transition state for electrocyclic and cycloaddition reactions involving phosphabutadienes is unfavorable. The former explanation appears most likely since cyclic phosphabutadienes are known to undergo pericyclic reactions.[46] We are continuing our efforts in this area and will report our results in due course.

Acknowledgment is made to the donors of the Petroleum Research Fund, administered by the American Chemical Society, for support of this research and to the National Science Foundation for equipment Grant DIR-8907135.

Registry No. 1-Aza-1,3-butadiene, 18295-52-8; 2-aza-1,3-butadiene, 38239-27-9; 1,3-diaza-1,3-butadiene, 35172-91-9; 1,4-diaza-1,3-butadiene, 40079-19-4; 2,3-diaza-1,3-butadiene, 503-27-5; 1-phospha-1,3-butadiene, 135865-42-8; 2-phospha-1,3-butadiene, 122682-85-3; 1,3-diphospha-1,3-butadiene, 134403-78-4; 1,4-diphospha-1,3-butadiene, 134403-79-5; 2,3-diphospha-1,3-butadiene, 122668-80-8.

Supplementary Material Available: Listings of Z matrices (HF/6-31G*) and energies of all critical points on the rotational surfaces of all compounds examined in this paper (10 pages). Ordering information is given on any current masthead page.

(46) (a) de Lauzon, G.; Charrier, C.; Bonnard, H.; Mathey, F.; Fischer, J.; Mitschler, A. *J. Chem. Soc., Chem. Commun.* **1982**, 1272-1273. (b) de Lauzon, G.; Charrier, C.; Bonnard, H.; Mathey, F. *Tetrahedron Lett.* **1982**, *23*, 511-514.

Ligand Field Strengths and Oxidation States from Manganese L-Edge Spectroscopy

S. P. Cramer,*[†,§§] F. M. F. deGroot,[§] Y. Ma,[‡] C. T. Chen,[‡] F. Sette,[‡] C. A. Kipke,[⊥] D. M. Eichhorn,[⊥] M. K. Chan,[⊥] W. H. Armstrong,[⊥] E. Libby,[‡‡] G. Christou,[‡‡] S. Brooker,[∥] V. McKee,[∥] O. C. Mullins,[††] and J. C. Fuggle[§]

Contribution from the Department of Applied Science, University of California, Davis, California 95616, AT&T Bell Laboratories, Murray Hill, New Jersey 07974, Department of Chemistry, Indiana University, Bloomington, Indiana 47405, Research Institute for Materials, University of Nijmegen, Toernooiveld, NL-6525 ED Nijmegen, The Netherlands, Schlumberger-Doll Research, Old Quarry Road, Ridgefield, Connecticut 06877, Department of Chemistry, University of California, Berkeley, California 94720, Department of Chemistry, Canterbury University, Christchurch, New Zealand, and Division of Applied Science, Lawrence Berkeley Laboratory, Berkeley, California 94720. *Received November 5, 1990*

Abstract: $L_{2,3}$ X-ray absorption spectra have been recorded for Mn(II), Mn(III), and Mn(IV) samples with a variety of ligands. For high-spin Mn(II) complexes, a systematic variation in spectra is observed as the ligand field is increased. A dramatically different spectrum is observed for $Mn(CN)_6^{4-}$, consistent with the presence of a low-spin complex. Progressing in oxidation state from Mn(II) to Mn(III) through Mn(IV) complexes, the primary peak position shifts first 1.5-2 eV and then 1-2 eV to higher energy, and the ratio of L_3 to L_2 intensity decreases. The spectra have been quantitatively simulated with an atomic multiplet program with an octahedral crystal field superimposed. The high resolution, strong sensitivity to chemical environment and amenability to quantitative spectral shape analysis indicate that L-edges of the first transition series metals are a potentially useful probe for bioinorganic studies.

Introduction

This paper presents new data on the chemical sensitivity of manganese $L_{2,3}$ X-ray-absorption edges and discusses the potential bioinorganic applications of soft X-ray L-edge spectroscopy. Transition-metal complex $L_{2,3}$-edge spectra involve 2p → 3d transitions and hence are sensitive to factors which change 3d orbital splittings and populations.[1] Improved synchrotron radiation beam lines allow these 3d metal L-edge spectra to be probed with high resolution,[2] and soft X-ray array detectors permit

[†] University of California, Davis.
[‡] AT&T Bell Laboratories.
[‡‡] Indiana University.
[§] University of Nijmegen.
[††] Schlumberger-Doll Research.
[⊥] University of California, Berkeley.
[∥] Canterbury University.
[§§] Lawrence Berkeley Laboratory.

Table I. X-ray Derived 10Dq vs Optical Values

Mn(II) complex	optical 10Dq (eV)	ref	X-ray 10Dq (eV)
$(Et_4N)_2[MnCl_4]$	-0.41	21	-0.30
MnS	0.88	22	0.60
$MnCl_2$	0.93	13	0.75
$MnCl_2$	1.03	14	
MnF_2	0.97	23	0.75
$MnSO_4$	~1.0	24	0.75
$(HB(3,5\text{-}Me_2pz)_3)_2Mn$	~1.3	24	1.05
$K_4Mn(CN)_6$	~3.7	26	3.90

0002-7863/91/1513-7937$02.50/0

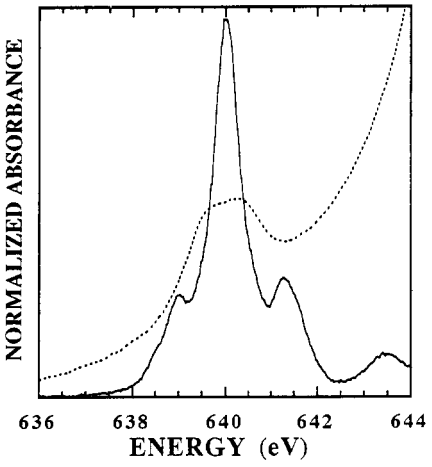

Figure 1. Comparison of K (--) and L_3 (—) edges for $MnCl_2$. The spectra have been arbitrarily aligned and only the 1s → 3d region of the K-edge is shown.

analysis of dilute metalloproteins.[3] In this communication, we illustrate the sensitivity of Mn L-edges to ligand field, spin state, and oxidation state, and we interpret the effects by performing atomic multiplet calculations including the cubic crystal field.

Experimental Section

L-edge spectra were recorded in electron yield mode with beam line U4-B[2] at the National Synchrotron Light Source. Finely powdered compounds were spread across the adhesive side of aluminum tape and placed with the sample normal at 45° to both the incoming beam and the vertical chamber axis. The sample chamber vacuum of better than 10^{-5} Torr was separated from the upstream vacuum of 10^{-10} Torr by a 1000 Å aluminum foil. A Galileo 4716 channeltron electron multiplier measured the electron yield from the sample as the monochromator swept the incident energy. The spectra were calibrated arbitrarily with 640 eV for the absorption maximum in MnF_2; the true value may be 1–2 eV lower.

MnF_2, MnO_2, $MnCl_2$, and $MnSO_4$ were used as received from Alfa Products. MnS was a kind gift from Dr. Russel Chiannelli, Exxon Research. $(NEt_4)_2MnCl_4$,[4] $K_4Mn(CN)_6$,[5] $(HB(3,5\text{-}Me_2pz)_3)_2Mn^{IV}(ClO_4)_2$,[6] $(HB(3,5\text{-}Me_2pz)_3)_2Mn^{III}(ClO_4)$,[7] $(HB(3,5\text{-}Me_2pz)_3)_2Mn^{II}$,[7] and $[Mn(acen)(NO_2)]$[8] were prepared in the Armstrong laboratory by the cited literature methods. $[Mn_2(HL)(Cl)_2]_2(ClO_4)_2\cdot 2dmf\cdot H_2O$[9] was prepared in the McKee laboratory, and $Mn_2O_2(pic)_4$[10] was prepared in the Christou laboratory.

Results and Discussion

The profound differences between 3d metal K- and L-edges are illustrated for $MnCl_2$ in Figure 1. A 1s → 3d transition is dipole-forbidden, and the weak doublet found at the foot of the K-edge is thought to occur both as a 1s → 3d quadrupole transition and by mixing of 4p character into the 3d band, by vibrations, or other means.[11,12] The splitting of 1.0 eV resolved in the second derivative spectrum is close to optical values of 0.93–1.03 eV reported for 10Dq.[13,14] In contrast with the simple and weak K-edge doublet, numerous strong features are observed at the L-edge.

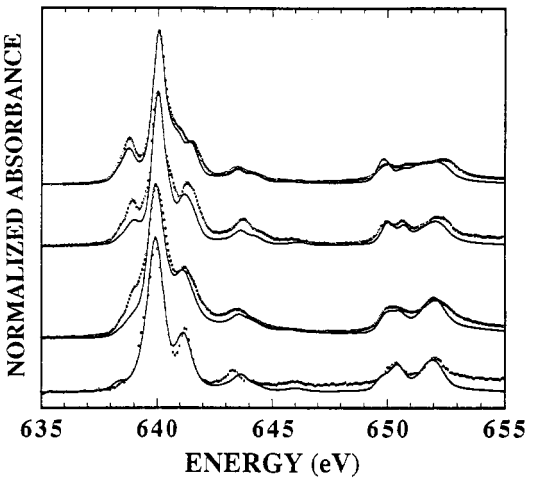

Figure 2. Experimental (OOO) and theoretical (—) $L_{2,3}$-edges for (top to bottom) $(HB(3,5\text{-}Me_2pz)_3)_2Mn$, MnF_2, MnS, and $[NEt_4]_2MnCl_4$. The 10Dq values used for the simulations are given in Table I. A Gaussian broadening of 0.1 eV was applied to correct for instrumental broadening. Additional Lorentzian line widths were applied to best simulate the data.

The additional structure has been interpreted as the combination of crystal field effects with splittings due to multipole 2p–3d and 3d–3d interactions. For the $Mn^{II}3d^5$ ion, the ^6S atomic ground state is determined by the multipole 3d–3d interactions, either factorized in Slater integrals (F^2,F^4) or alternatively in Racah parameters (B,C). The ^6S atomic ground state does not split; in cubic symmetry the fully symmetric state is renamed to $^6A_1$. From this $^6A_1(2p^63d^5[(t_{2g}^{+3}(e_g^+)^2])$ ground state, transitions are possible to a series of $2p^53d^6$ final states of symmetries which couple to the ground state. The final states are, like the ground state, determined by the 3d–3d multipole interactions. Important additional interactions are caused by the core hole: the 2p core hole spin-orbit coupling splits the absorption spectrum into an L_3 and an L_2 part, and the 2p–3d multipole Coulomb and exchange interactions (F^2,G^1,G^3), which are on the order of 5 eV, also modify the spectrum considerably. This gives rise to hundreds of lines with distinct envelopes.[15]

An important factor for the broadening of the line spectrum is the lifetime of the final state. Depending on the specific symmetry of the final state, the possible (Auger) decay channels have different transition probabilities and lifetimes. As these symmetry-dependent relaxation rates are unknown, for the simulations all lines are broadened equivalently with a Lorentzian of 0.1 eV for the L_3 edge and 0.3 eV for the L_2 edge.

Experimental L-edge spectra for a series of octahedral Mn(II) complexes are compared with atomic multiplet calculations in Figure 2. For these calculations, atomic values for the Slater integrals were used.[16] The values of 10Dq which gave the best simulations are compared with parameters derived from UV–visible spectroscopy in Table I. It reveals that there is a deviation between the UV–visible and X-ray results. The 10Dq values from X-ray absorption, which in fact are final state values, are approximately 25% smaller than the UV–visible results. This relation

(1) Fuggle, J. C. *Physica Scr.* **1987**, *T17*, 64–69.
(2) (a) Chen, C. T. *Nucl. Inst. Meth.* **1987**, *A256*, 595–604. (b) Chen, C. T.; Sette, F. *Rev. Sci. Instr.* **1989**, *60*, 1616.
(3) Cramer, S. P.; Tench, O.; Yocum, M.; Kraner, H.; Rogers, L.; Radeka, V.; Mullins, O.; Rescia, S. *X-ray Absorption Fine Structure—Proceedings of the 6th International XAFS Conference* Hasnain, S. S., Ed.; Ellis Horwood Chichester 1991; pp 640–645.
(4) Gill, N. S.; Taylor, F. B. *Inorg. Synth.* **1967**, *9*, 136.
(5) Meyer, J. *Z. Anorg. Chem.* **1913**, *81, 385–405.
(6) Chan, M. K.; Armstrong, W. H. *Inorg. Chem.* **1989**, *28*, 3777.
(7) Chan, M. K.; Armstrong, W. H., manuscript in preparation.
(8) Boucher, L. J.; Day, V. W. *Inorg. Chem.* **1977**, *16*, 1360.
(9) Brooker, S.; McKee, V. *J. Chem. Soc., Chem. Commun.* **1989**, 619.
(10) Christou, G. *Acc. Chem. Res.* **1989**, *22*, 328–335.
(11) (a) Hahn, J. E.; Hodgson, K. O. In *Inorganic Chemistry: Towards the 21st Century*; Chisholm, M. H., Ed.; ACS Symposium Series, Vol. 211, New York, 1983; pp 431–444. (b) Hahn, J. E.; Scott, R. A.; Hodgson, K. O.; Doniach, S.; Desjardins, S. R.; Solomon, E. I. *Chem. Phys. Lett.* **1982**, *88*, 595–598.
(12) Poumellec, B.; Cortes, R.; Tourillon, G.; Berthon, J. *Conference Proceedings Vol 25: 2nd European Conference on Progress in X-ray Synchrotron Radiation Research*; Balerna, A., Bernieri, E., Mobilio, S., Eds.; SIF: Bologna, 1990.
(13) Pappalardo, R. *J. Chem. Phys.* **1959**, *31*, 1050–1061.
(14) Stout, J. W. *J. Chem. Phys.* **1960**, *33*, 303.
(15) deGroot, F. M. F.; Fuggle, J. C.; Thole, B. T.; Sawatzky, G. A. *Phys. Rev. B* **1990**, *41*, 928–937. deGroot, F. M. F.; Fuggle, J. C.; Thole, B. T.; Sawatzky, G. A. *Phys. Rev. B* **1990**, *42*, 5459–5468.
(16) The atomic values for the Slater integrals were calculated ab initio within the Hartree–Fock limit with Cowan's RCN program. To account for intraatomic configuration interaction the Hartree–Fock values were reduced to 80%. See: Cowan, R. D. In *The Theory of Atomic Structure and Spectra*; University of California Press: Berkeley, 1981; p 464, and references therein.

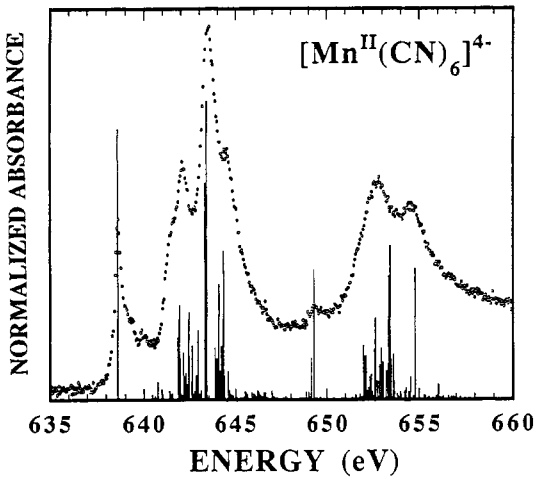

Figure 3. Experimental (OOO) $L_{2,3}$-edge spectrum for $K_4Mn(CN)_6$, compared with the stick diagram showing relative oscillator strengths of individual transitions before instrumental and line width broadening, calculated with 10Dq = 3.9 eV.

is valid for all high-spin Mn(II) complexes. The decrease of the cubic crystal field strength in the final state may be due to an increased localization of the 3d states in the presence of the core hole.[17] A similar argument would appear to hold for the K-edge splittings, yet these appear comparable to the optical values. Further study of the relationship between X-ray and optical splittings is clearly needed.

The branching ratio of L_3 edge intensity to total line strength, $I(L_3)/I(L_3 + L_2)$, decreases significantly for low-spin Mn(II), as illustrated by the spectrum of $Mn(CN)_6^{4-}$ in Figure 3. Such changes have been theoretically analyzed by Thole and van der Laan.[18] For Mn(II) the theoretical branching ratio is 0.75 for high-spin and 0.59 for low-spin. A crystal field multiplet calculation with an octahedral crystal field strength of 3.9 eV results in a $^2T_2(3d^5[(t_{2g}^+)^3(t_{2g}^-)^2])$ ground state. From this ground state, transitions are possible to $2p^53d^6$ final states where the six d electrons have $^1A_1[(t_{2g}^+)^3(t_{2g}^-)^3]$ symmetry. For the L_3 region, this state is separated by about 2 eV from the other $2p^53d^6$ multiplet lines. Examination of the low energy side of this band reveals a line width of ~0.35 eV.

Significant changes in L-edge structure and position occur upon oxidation from Mn(II) to Mn(III) or Mn(IV), as shown in Figure 4. For complexes with the same ligands, the average shift in main peak position is on the order of 1.5–2 eV for Mn(II) to Mn(III) and about 1–2 eV for Mn(III) to Mn(IV). For comparison, Mn K-edges shift on the order of 3–4 eV for similar oxidation state changes.[19] Since the reported natural line widths for K- and L-edges are 1.12 and 0.32 eV, respectively,[20] it appears that the ratio of edge shift to resolution is higher for the L-edges. This should make L-edges more favorable for deciphering mixtures of oxidation states.

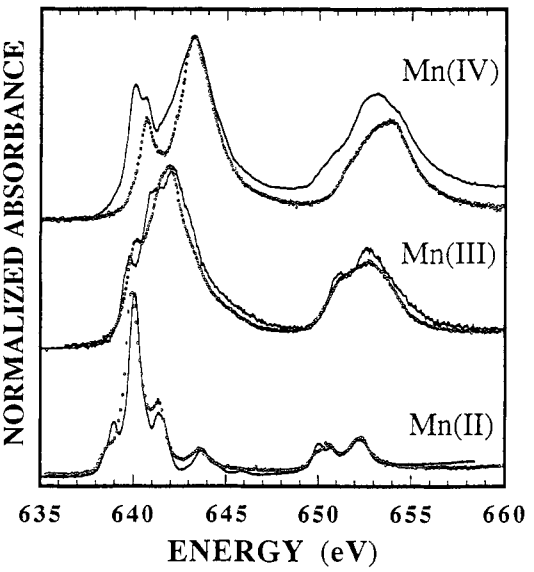

Figure 4. Oxidation data dependence of L-edge position and shape. Top to bottom: $(HB(3,5\text{-}Me_2pz)_3)_2Mn^{IV}(ClO_4)_2$ (—) and $Mn(^{IV})_2O_2(pic)_4$ (•••), where pic = picolinate anion; piemontite-$Ca_2(Mn^{III},Fe^{III},Al)_2AlO\cdot OH[Si_2O_7][SiO_4]$ (—) and $Mn^{III}(acen)(NO_2)$ (•••), where acen = *N*,*N*′-ethylenebis(acetylacetone imine); $Mn^{II}Fe_2$ (—) and $[Mn^{II}_2(HL)(Cl)_2]_2(ClO_4)_2\cdot 2dmf\cdot H_2O$ (•••), where H_2L = 1,7,14,20-tetramethyl-2,6,15,19-tetraaza[7,7](2,6)-pyridinophane-4,17-diol. The spectrum of the first Mn(IV) complex appears to be contaminated by a small amount of its Mn(II) precursor complex. Energy calibration arbitrarily used MnF_2 maximum as 640 eV.

In the present simulations it is assumed that the Mn(II) ion exists as a pure $3d^5$ ground state. For a higher oxidation state such as Mn(IV), assumption of the corresponding $3d^3$ ground state is less justified. Due to increased covalency, mixing of $3d^4\underline{L}$ character, where $\underline{L}$ means a hole on the ligand, is more important. In the present calculations the role of covalency is not considered explicitly, but the effects are effectively included by reducing the Slater integrals.

An additional complicating factor for high-spin Mn(III) spectra is that the $^5E - 3d^4[(t_{2g}^+)^3(e_g^+)^1]$ ground state in octahedral symmetry is not stable because of the half-filled e_g level. This degeneracy is lifted by a Jahn–Teller distortion which reduces the symmetry to tetragonal. Preliminary investigation reveals lower symmetry can have a considerable effect on the spectra. In summary, although the simulations of ionic Mn(II) complexes were successful, additional work is needed to assess the utility of the atomic multiplet model for lower symmetry and more covalent Mn(III) and Mn(IV) complexes.

Conclusions and Prognosis

Since K level near edge and EXAFS spectroscopies are now popular tools for bioinorganic studies, it is worth noting the potential of $L_{2,3}$ edges for first transition-metal characterization in biological samples.[29] A dominant experimental factor is the short penetration length of L-edge X-rays. In the 500–1000 eV range where vanadium through zinc L-edges occur, most absorption coefficients are 2–3 orders of magnitude higher than at K-edge energies. Thus, for example, the 1/e transmission length in aqueous media is 7800 Å at the Mn L-edge, compared to 0.4 mm at 6 keV near the Mn K-edge. This requires dramatic changes in sample handling, window technology, and detectors. Also, the $L_{2,3}$ fluorescence yields are 0.3–1%,[31] 50–100 times lower than

(17) Gunnarson, O.; Andersen, O. K.; Jepsen, O.; Zaanen, J. In Core-Level Spectroscopy in Condensed Systems; Kanamori, J., Kotani, A., Eds.; Springer Series in Solid State Science, Springer-Verlag: Berlin Vol. 81, 1988; p 82.
(18) Thole, B. T.; van der Laan, G. *Phys. Rev. B* **1988**, *38*, 3158–3171.
(19) Penner-Hahn, J. E.; Fronko, R. M.; Pecoraro, V. L.; Yocum, C. F.; Betts, S. D.; Bowlby, S. R. *J. Am. Chem. Soc.* **1990**, *112*, 2549–2557.
(20) Krause, M. O.; Oliver, J. H. *J. Chem. Phys. Ref. Data* **1979**, *8*, 329–337.
(21) Vala, M. T.; Ballhausen, C. J.; Dingle, R.; Holt, S. L. *Mol. Phys.* **1972**, *23*, 217–234.
(22) Jorgenson, C. K. *Struct. Bonding* **1966**, *1*, 1–31.
(23) Stout, J. W. *J. Chem. Phys.* **1959**, *31*, 709–719.
(24) Approximate values for 10Dq were estimated with Jorgenson's relation $10Dq \cong f\cdot g\cdot 10^3$ cm^{-1}.[25] For Mn(II) complexes we used $g \cong 8.0$; for $MnSO_4$ we assumed $f \cong 1.3$ (based on the value reported for SO_3^{2-}), and for the trispyrazoylborate complex we used $f \cong 1.43$ (based on the value reported for *o*-phenanthroline).[27]
(25) (a) Jorgenson, C. K. *Absorption Spectra and Chemical Bonding in Complexes*; Pergamon Press: Oxford, 1962. (b) Jorgenson, C. K. *Modern Aspects of Ligand Field Theory*; North Holland: Amsterdam, 1971.
(26) Alexander, J. J.; Gray, H. B. *J. Am. Chem. Soc.* **1968**, *90*, 4260–4271.
(27) (a) *Introduction to Ligand Fields*; Figgis, B. N., Ed.; John Wiley: New York, 1966; p 244. (b) Lever, A. P. B. *Inorganic Electronic Spectroscopy*; Elsevier: Amsterdam, 1984; p 748.
(28) Thole, B. T.; Cowan, R. D.; Sawatzky, G. A.; Fink, J.; Fuggle, J. C. *Phys. Rev.* **1985**, *B31*, 6856.
(29) Preliminary spectra for the blue copper protein stellacyanin[3] and the Fe–S protein rubredoxin[30] have already been reported.
(30) George, S.; Chien, J.; Cramer S. P. *NSLS Activity Report*; 1990.

the K-edge yields. Fortunately, the background signal from Compton scattering is small at L-edge energies. Although the overall experimental sensitivity may be lower, the signal-to-noise requirements for edge analysis are less stringent than for EXAFS, and as the technology improves, obtaining these spectra will no doubt eventually become routine.

Compared to the broad K-edge features, the sharper and richer $L_{2,3}$-edge multiplet structure appears more amenable to resolving the presence of mixtures of oxidation states, although this remains to be proven. For spectroscopic determination of interatomic distances, K-edge EXAFS is not challenged by 3d metal L-edge EXAFS, because several hundred volts of uninterrupted oscillations are generally required, and too many overlapping and interfering edges occur in the soft X-ray region. However, for detecting small changes in the transition-metal site symmetry, the sharper $L_{2,3}$ edge spectra may be more sensitive and more quantitatively interpretable than the K-edge data. The confluence of better sources, monochromators, detectors, and theoretical procedures makes soft X-ray spectroscopy a promising new tool for bioinorganic problems.

Acknowledgment. We thank Dr. Theo Thole and Prof. George Sawatzky for helpful discussions and for making their simulation software available. Dr. Andrew Campbell and Prof. Roger Burns of MIT are gratefully acknowledged for the piemontite sample. This work was partially supported by the National Institutes of Health, Grants GM-44380 (to S.P.C.) and GM-38275-01 (to W.H.A.). W.H.A. also acknowledges funding from the Searle Scholars and the National Science Foundation Presidential Young Investigators Programs. The National Synchrotron Light Source is funded by the Department of Energy, Office of Basic Energy Sciences.

(31) Krause, M. O. *J. Chem. Phys. Ref. Data* **1979**, *8*, *1979*, 307-327.
(32) Lynch, D. W.; Cowan, R. *Phys. Rev.* **1987**, *B36*, 9228.

From 1-D to 3-D Ferrimagnets in the EDTA Family: Magnetic Characterization of the Tetrahydrate Series $M^tM(M'EDTA)_2 \cdot 4H_2O$ [M^t, M, M′ = Co(II), Ni(II), Zn(II)]

F. Sapiña,*,† E. Coronado,*,† D. Beltrán,† and R. Burriel‡

Contribution from the Departamento de Quimica Inorgânica, Facultad de Ciencias Quimicas, Universidad de Valencia, 46100 Burjassot, Spain, and Instituto de Ciencia de Materiales de Aragôn, CSIC-Universidad de Zaragoza, 50009 Zaragoza, Spain. *Received March 22, 1991*

Abstract: We report on the magnetic behavior of the compounds $M^tM(M'EDTA)_2 \cdot 4H_2O$ (in short [M^tMM']) in the very low temperature range. The structure of these compounds can be formally regarded as ordered bimetallic layers of alternating chelated and hydrated octahedral sites M and M′, with tetrahedral sites M^t connecting different MM′ layers. We have obtained the compounds [ZnZnNi], [ZnNiNi], [CoNiNi], [CoCoNi], and [CoCoCo]. While the compound [ZnNiNi] may support a 2-D magnetic lattice of Ni(II), since Zn(II) occupies tetrahedral sites, in the compounds without Zn the layers are connected through Co(II), increasing the dimensionality of the lattice to 3-D. A leveling of the magnetic susceptibility has been observed in [ZnNiNi], which has been attributed to zero-field splitting effects of the chelated Ni(II) ions. On the other hand, as expected on the basis of the structure, the substitution of Zn(II) by Co(II) in the tetrahedral site leads to the appearance of 3-D ferrimagnetic interactions in the compounds [CoNiNi], [CoCoNi], and [CoCoCo]. This is clearly noticeable from the sharp transition temperatures in the first two compounds at T_c = 0.44 and 0.10 K, respectively, with an out-of-phase susceptibility signal below T_c. In [CoCoNi], there is a rounded maximum in the $\chi_m T$ plot at T = 0.40 K. The magnetic data in the low-dimensional region have been analyzed for the compounds [CoCoCo] and [CoCoNi] by means of an anisotropic (Ising-type) model that assumes three different magnetic sublattices exchange-coupled by two magnetic interactions, as well as the local anisotropies of tetrahedral Co(II) and chelated Ni(II) ions.

Introduction

Major progress is being made by chemists in preparing novel low-dimensional magnetic materials in which two magnetic sublattices of unequal magnitude are structurally ordered. Thus, there are a variety of new bimetallic materials in which the different metal ions are chemically ordered, in particular the so-called ferrimagnetic chains or 1-D ferrimagnets. These compounds are desirable because they may have distinctive magnetic properties associated with the inability of the antiferromagnetic interaction to cancel the opposing unequal moments.[1] Further, they provide starting blocks from which to synthesize molecular-based ferromagnets, i.e., compounds having spontaneous magnetization below a critical temperature. This has been found when 1-D ferrimagnets are assembled in a ferromagnetic fashion taking advantage of the dipolar interchain interactions.[2,3] Such an approach is clearly limited by the chemical inability to control the relative positions of chains on the lattice scale, as well as by the weakness of the interchain interactions. A much more promising approach consists of connecting the chains by covalent bonds (instead of hydrogen bonds) in order to obtain 2-D or 3-D ordered bimetallic lattices.

Our own contribution in this area has dealt with the synthesis and magneto–structural chemistry of an extensive series of ordered bimetallic materials, namely the EDTA family.[4] We have shown the usefulness of EDTA and EDTA-like ligands in the preparation

†Universidad de Valencia.
‡CSIC-Universidad de Zaragoza.

(1) Landee, C. P. In *Organic and Inorganic Low Dimensional Crystalline Materials*; Delhaes, P., Drillon, M., Eds.; NATO ASI Series 168; Plenum Press: New York, 1987; p 75.
(2) Kahn, O. In *Organic and Inorganic Low Dimensional Crystalline Materials*; Delhaes, P., Drillon, M., Eds.; NATO ASI Series 168; Plenum Press: New York, 1987; p 93.
(3) Caneschi, A.; Gatteschi, D.; Sessoli, R.; Rey, P. *Acc. Chem. Res.* **1989**, *22*, 392.
(4) Coronado, E. In *Magnetic Molecular Materials*; Gatteschi, D., Kahn, O., Miller, J. S., Palacio, F., Eds.; NATO ASI Series 198; Kluwer Academic Publishers, 1991; p 267.

0002-7863/91/1513-7940$02.50/0